Strong double-layer formation by shock waves in nonequilibrium plasmas

P. Bletzinger,* B. N. Ganguly,† and A. Garscadden
Air Force Research Laboratory, Wright-Patterson Air Force Base, Ohio 45433-7919
(Received 14 February 2002; revised manuscript received 25 October 2002; published 28 April 2003)

Strong double-layer formation by acoustic shock wave ($<$M$=2$) propagation in a low-pressure, N_2 positive column plasma has been quantified, near the shock front, by measurements of the voltage jump and the enhancements of both the $B\ ^3\Pi_g - A\ ^3\Sigma_u^+$ plasma emission and the electron density. The large polarity dependence (or shock direction) of these effects and potential jumps of more than $20kT_e$ across the shock-created interface indicate that the measured shock-induced electron heating effects (localized excitation and ionization rate) are caused by the formation of *strong* double layers maintained by the traveling shock front.

DOI: 10.1103/PhysRevE.67.047401 PACS number(s): 52.50.Lp, 47.40.Nm, 52.70.Gw

Previous studies have shown that gas dynamic shock propagation through a plasma locally polarizes the plasma, and forms space-charge layers at the shock front [1–3]. The shock wave propagation produces a discontinuous jump in the neutral density. In a weakly ionized dc discharge, this neutral density jump creates associated discontinuities in the electron temperature and electron density. It has been shown that a double layer forms at such an interface and that the strength of double-layer formation is determined by the mean electron temperature differences between the plasmas [4–6]. The potential jump across a current-free stationary double layer, separating plasmas with two different mean electron energies [4], is limited to about $2kT_e$, which is in agreement with the previously calculated potential jump across a gas dynamic shock front [2,3]. However, under our experimental conditions with current flow, we measure very large potential jumps across the shock. In this work, we present the evidence for the formation of a traveling *strong* double layer near the shock front for shock propagations through a nonequilibrium ($T_e \gg T_i$) glow discharge plasma. The existence of a strong double layer with a significant potential jump leads to local electron heating [5–8], excitation, ionization, and local gas heating. The last effect contributes to shock broadening and velocity change in addition to the effect of overall discharge heating [9–11]. The detailed application of plasmas in the aerodynamics of flight is described in a recent review article [12].

In this paper, we report measurements of the formation of a moving (faster than ion thermal speed) strong double layer when a weak acoustic shock wave ($<$M$=2$) propagates through a low-pressure (3–5 Torr), low-current-density (2–5 mA/cm^2), N_2 positive column plasma. An electric-spark-driven shock tube is used to generate shock waves, and the shock-wave-induced modulations of the plasma properties are measured in a 3 cm diameter discharge tube with glass wall conformal electrodes spaced 20 cm apart shown in Fig. 1. The experimental details are described elsewhere [13]. The shock-induced double-layer strength is determined using a pair of floating probes, spaced 2 cm apart axially; the floating voltage differential is used to measure the potential jump across the shock front. The probe time response is limited by the response time of the probe sheath and the circuit capacitance of the high-impedance circuit. Since the electron temperatures before and after the shock front are relatively close (1 and 0.3 eV), the floating potential difference is a good approximation of the plasma potential difference. The evidence of local electron heating by the strong double layer is obtained from measurement of the enhancements of direct electron impact excitation and of ionization. The excitation enhancement is measured by using a photomultiplier with a narrowband spectral filter to select the $B\ ^3\Pi_g - A\ ^3\Sigma_u^+$ (0,2) transition at 775.4 nm. A 100 mm focal length lens with F 30 optics is used to obtain 1.7 mm spatial resolution over the 30 mm radial plasma column. The electron density on both sides of the shock discontinuity is measured using an X-band (8 GHz) microwave interferometer with a pair of 30 cm diameter focusing mirrors coupled to a pair of standard gain horns. This transmit-receive microwave beam arrangement provides 4 cm spatial resolution at the beam waist, which is adequate for comparison of the electron densities on both sides of the shock discontinuity. The arrival of the shock wave in the viewing volume of the plasma emission, floating probes, and microwave beam is measured by a colocated photodeflection laser beam [13].

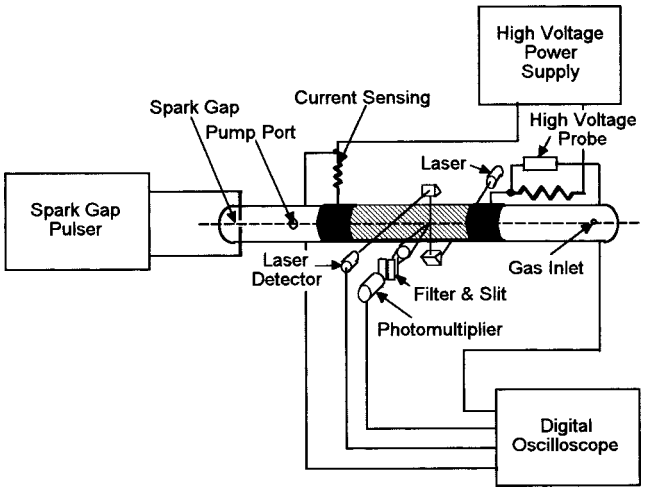

FIG. 1. Schematic of experiment. In an alternative setup, the photomultiplier and filter are replaced by the transmit/receive antennas of a microwave interferometer.

*Present address: ISSI, Dayton, OH 45440.
†Email address: Biswa.ganguly@wpafb.af.mil

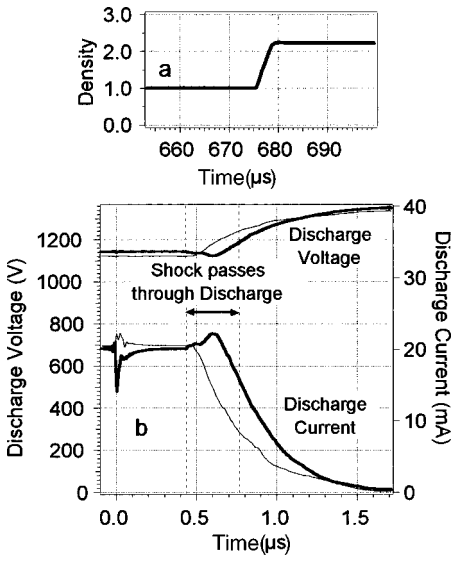

FIG. 2. (a) Integrated photodeflection signal showing the normalized neutral density jump at the shock front for M 1.76 shock wave. (b) Discharge voltage and current in a 3 Torr, 20 mA discharge in N_2 for a shock propagating from cathode to anode (thick curves) and anode to cathode (thin curves). The time during which the shock traverses the 20 cm long discharge is indicated by the vertical dashed lines. The spark discharge generating the shock wave is at 0 ms.

Figure 2(a) shows the normalized neutral density jump (integrated photodeflection signal) [9,13] for a M 1.76 shock front as it moves through the positive column. The photodeflection laser beam is located at the same position in the positive column as the photomultiplier. The neutral density increases by a factor of 2.2 behind the M 1.76 shock front. Figure 2(b) shows the shock-induced modulation of discharge voltage and current for both cathode to anode and anode to cathode shock propagation directions. The gas pressure was 3 Torr, the discharge current 20 mA. The shock wave velocity was M 1.76. The time period during which the shock wave traverses the discharge is indicated by the vertical dashed lines. As observed previously [13], the global effects of the shock were that the discharge voltage decreases and the current increases by 10% for about 100 μs for cathode to anode shock propagation direction; for the opposite propagation direction the voltage increases and the current decreases immediately. The decay of the discharge current after the shock exits the plasma region is exponential. The *B*-*A* plasma emission, shown in Fig. 3, indicates that locally at the photomultiplier observation point the light intensity increases when the shock wave enters the discharge for cathode to anode propagation and decreases for the opposite propagation direction. The electrical and the plasma emission effects, before arrival of the shock at the observation point, are caused by the global electrical circuit response to the propagating shock wave [13]. A sharp and pronounced peak of 775.4 nm emission is observed when the shock wave passes through the observation region for both propagation directions. The emission peaks have a rise time of 2 μs and a decay time of about 40 μs. The long decay time is probably caused by the heavy-particle-collision-induced excitation

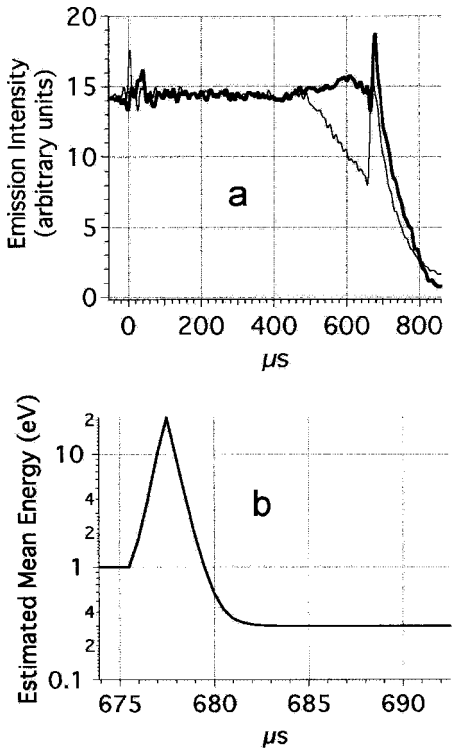

FIG. 3. (a) Spatially and temporally resolved 775.4 nm emission under the same discharge condition as in Fig. 2 at approximately the center of the discharge for the two directions of shock propagation. (b) Local mean electron energy during shock transition as estimated from the excitation rate derived from the 775.4 nm emission intensity.

[14] of the B state due to the reaction $N_2(A\ ^3\Sigma_u^+) + N_2(X\ ^1\Sigma_g^+,\ v \geqslant 5) \rightarrow N_2(B\ ^3\Pi_g) + N_2(X\ ^1\Sigma_g^+)$. (Both the $A\ ^3\Sigma_u^+$ state and the vibrationally excited ground state have long lifetimes.) The rapid rise in intensities of the 775.4 nm emission is an indicator of a large increase in electron impact excitation rate connected with the shock-wave-induced very local increase in E/n value (or electron mean energy). Due to the resolution limits of the optical system, the temporal width of the rising portion of the measured 775.4 nm radiation pulses, which corresponds to the apparent duration of the shock-wave-generated local transient increase in E/n, is much longer than the actual width of these radiation pulses and also the duration of the increased electronic excitation. For the same reason, the amplitudes of the measured pulses are much smaller than the actual radiation amplitudes. For this positive column discharge [15,16], which runs at $E/n \approx 45$ Td ($1\ \mathrm{Td} = 1 \times 10^{-17}\ \mathrm{V\,cm^2}$) with mean electron temperature ≈ 1 eV, the observed $B\ ^3\Pi_g - A\ ^3\Sigma_u^+$ intensity jumps in 2 μs by at least 20% compared to the steady state. This requires a rate of change of the electron impact excitation by a factor of 10^5 (20% change from the steady state emission intensity in 2 μs). For an equivalent steady state this result would require that the E/n increases [15,16] from 45 to more than 240 Td. In fact, the rapid field change translates the electron energy distribution instantaneously to higher energy. We estimate that a change of 10 eV is sufficient to produce the observed excitation [Fig. 3(b)]. The de-

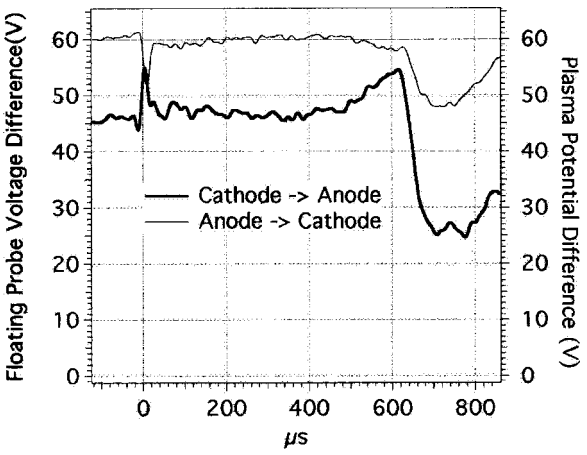

FIG. 4. Difference of floating probe signals from a 60 mA discharge in N_2 at 5 Torr for the two directions of shock propagation.

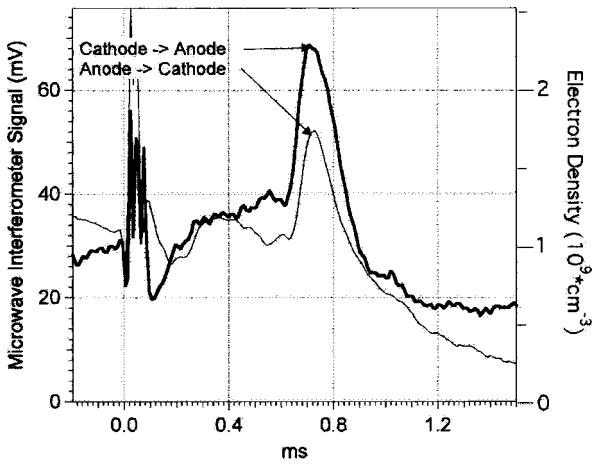

FIG. 5. Microwave interferometer signals for a 3 Torr, 60 mA N_2 discharge and a M 1.6 shock wave for the two directions of propagation. The steady state interferometer signal is about 24 mV.

cay of the 775.4 nm radiation is strictly due to the population transfer from long-lived states after the short period of direct electron impact excitation enhancement; no such long decay was observed with the 337.1 nm radiation [13] since the C state is populated primarily by direct electron impact. Figure 4 shows shock-wave-induced floating probe differential voltage changes for a 5 Torr, 60 mA discharge. Similar to the discharge voltage and 775.4 nm emission behavior, the electric field at the probe location rises for the cathode to anode propagation direction and decreases for the opposite direction before shock arrival. However, when the shock wave passes through the probe location, in both directions a large voltage drop is observed. The sudden drop in the voltage amounts to 25 V in cathode to anode directed shock propagation and 9.5 V in the opposite propagation direction. The absolute accuracy of these voltage changes [17] is $\pm 30\%$. Considering the measured voltage drops and the spatial dimension over which they occur, these voltage jumps across the shock front are more than $20kT_e$ (where kT_e is the mean electron energy of the unperturbed plasma), which by Poisson's equation requires the formation of strong double layers at the shock front. The high electric fields in this very localized space-charge region (dimension determined by the electron Debye length), ahead of the shock front, then lead to the enhancement of local excitation and ionization; the latter creates a much higher electron density behind the shock than in the unperturbed plasma. The optical measurements indicate the enhanced electron impact excitation at the shock front. In order to quantify the enhanced ionization, the electron density was measured with the microwave interferometer. Results are shown in Fig. 5 for the two directions of shock wave propagation. The measured increase in electron density is 150% for the cathode to anode direction. Note that the actual ionization rise time will be similar to the excitation rise time, shown in Fig. 3, which is much faster than the temporal response shown in Fig. 5.

The optical, microwave, and electrical measurements give a self-consistent picture of the plasma–shock-wave interactions and the measurements reported provide evidence for the presence of strong excitation (and ionization) enhancement in a very narrow region propagating with the shock wave for initially weakly ionized plasmas. These measurements provide direct evidence of the formation of strong double layers in collisional shock wave propagation in nonequilibrium plasmas. The double layer formed under our measurement conditions is a transient moving double layer traveling faster than the ion sound speed and, therefore, theory indicates [5–7] that it can support a strong space-charge layer with a potential jump $\geqslant 10kT_e$.

The discharge current continuity requirement across the shock front imposes additional constraints on the electron and ion flux continuity conditions. The local transient electric field is additive to the steady state plasma electric field in the cathode to anode shock propagation direction and it is subtractive in the opposite direction, leading to a polarity dependence of the double-layer voltage jump [18,19].

In conclusion, we have provided direct evidence for the large jump in plasma potential, the fast increase of electron excitation temperature as indicated by the sudden increase in the emission rate, and the increase in n_e caused by the formation of strong double layers, at the shock front, in nonequilibrium plasmas. One of the important implications of the strong-double-layer-induced local electron heating is that a very localized energy deposition and gas heating at the shock front is possible so that shock wave dispersions and modifications of shock jump conditions cannot always be determined from the steady state or spatially averaged gas properties [9–11].

[1] M. Y. Jaffrin and R. F. Probstein, Phys. Fluids **7**, 1658 (1964).
[2] M. Y. Jaffrin, Phys. Fluids **8**, 606 (1965).
[3] M. A. Liberman and A. L. Velikovich, *Physics of Shock Waves in Gases and Plasmas* (Springer, New York, 1985), pp. 91–128.
[4] S. Ishiguro, T. Kamimura, and T. Sato, Phys. Fluids **28**, 2100 (1985).
[5] N. Hershkowitz, Space Sci. Rev. **41**, 351 (1985).
[6] M. A. Raadu, Phys. Rep. **178**, 25 (1989), and references therein.
[7] C. Chan, N. Hershkowitz, and K. E. Lonngren, Phys. Fluids **26**, 1587 (1983).
[8] L. Conde, L. F. Ibanez, and C. Ferro-Fontan, Phys. Rev. E **64**, 046402 (2001).
[9] P. Bletzinger and B. N. Ganguly, Phys. Lett. A **258**, 342 (1999).
[10] A. S. Baryshnikov, I. V. Basargin, and M. V. Chistyakova, Tech. Phys. **46**, 287 (2001).
[11] D. Bivolaru and S. P. Kuo, Phys. Plasmas **9**, 721 (2002).
[12] A. F. Alexandrov, N. V. Ardelyan, S. N. Chuvashev, A. P. Ershov, A. A. Rukhadze, I. B. Timofeev, and V. M. Shibkov, J. Tech. Phys. **41**, 533 (2000), special issue.
[13] P. Bletzinger, B. N. Ganguly, and A. Garscadden, Phys. Plasmas **7**, 4341 (2000).
[14] L. G. Piper, K. W. Holtzclaw, and B. D. Green, J. Chem. Phys. **90**, 5337 (1989).
[15] K. Behringer and U. Fantz, J. Phys. D **27**, 2128 (1994).
[16] J. Lourerio and C. M. Ferreira, J. Phys. D **22**, 67 (1989).
[17] The voltage drops cannot simply be interpreted as a linear voltage differential between the floating probes over the distance between the probes. Instead, they represent the gradual voltage change when a space-charge layer moves between two probes, inducing potential changes. This hypothesis was verified by using three equally axially spaced probes and comparing the voltage differentials between probes 1 and 2, 2 and 3, and then 1 and 3. The voltage drop between probes 1 and 3 was no larger than the voltage drops between the other configurations, but the temporal width was twice as long. Therefore, the measured voltage differentials are caused by a very thin space-charge layer, estimated to be no thicker than 1 mm from the optical emission measurements, propagating with the shock front.
[18] H. S. Maciel and J. E. Allen, J. Plasma Phys. **42**, 321 (1989).
[19] J. M. Williamson and B. N. Ganguly, Phys. Rev. E **64**, 036403 (2001).